Research Article

Xiaokai Wu, Dingbo Shu, Shaowen Huang, Chunping Yang, Bo Li, Shengnan Huang, Juan Li*, and Xiaogang Yin*

Preparation of maleic anhydride-modified curcumin/PBAT composite film for food packaging

https://doi.org/10.1515/epoly-2024-0087
received August 27, 2024; accepted December 16, 2024

Abstract: Polybutylene adipate terephthalate (PBAT) is popular due to its low cost, good biodegradability, and excellent mechanical properties. Maleic anhydride (SMA) can easily graft with curcumin (CUR), a substance known for its antibacterial and antioxidant properties, acting as a nucleating agent with high dispersibility, which has led to the successful production of the functional modifier CUR −SMA. This research involves the creation of PBAT composite films with various weight percentages of CUR−SMA (0.1, 0.3, 0.5, 0.7, and 0.9% w/w) using extrusion and blow molding techniques. The research chemically links CUR and SMA to form a robust and cohesive composite material. The study investigates the structure, mechanical properties, water vapor barrier capabilities, oxygen barrier properties, fracture morphologies, antibacterial and antioxidant properties, and biodegradability, as well as the freshness-preserving impact of the film. The composite shows an excellent effect, surpassing that of single-component blends, by minimizing CUR−SMA migration, enhancing mechanical properties, and increasing the barrier characteristics of composite films. The interaction between CUR−SMA and PBAT results in the formation of a cross-linked network structure through chain extension reactions. The tensile strength increased by 56%, from 17.5 to 27.3 MPa. The antioxidant activity reached up to 72.26%. The films exhibit significant antibacterial properties against *Staphylococcus aureus*. The films retain the biodegradability of PBAT. The PBAT/CUR−SMA films have successfully enhanced the shelf life of oyster mushrooms, strawberries, and apples due to their strong antioxidant, antibacterial, and waterproof qualities.

Keywords: poly(butylene adipate-co-terephthalate), curcumin, maleic anhydride, composite packaging film, antibacterial activity

1 Introduction

Fresh produce has a very short shelf life and is vulnerable to rot and mold during storage and shipping, which endangers food safety and edibility (1). Consequently, it is imperative to extend the shelf life of fruits and vegetables using efficient techniques, and plastic wrap is regarded as an affordable and efficient option among the many available methods. Food deterioration due to oxidation reactions and microbiological growth cannot be addressed by relying solely on a single food packaging film (2,3). The development of food packaging is now focusing on multifunctional composite materials made of biodegradable polymers, particularly in the study and use of antibacterial membranes (4). To extend the shelf life of fruits and vegetables, the research of biodegradable films with strong machinery and antioxidants in food packaging applications is more concerned by researchers than conventional polymers (5). For food packaging, polybutylene adipate terephthalate (PBAT) is the best material. It is a copolymer of aliphatic and aromatic chemicals, is completely biodegradable and biocompatible, and

* **Corresponding author: Juan Li,** R&D Department, Guizhou Material Industrial Technology Institute, Guiyang, 550014, China; College of Materials and Metallurgy, Guizhou University, Guiyang, 550025, China, e-mail: 970028280@qq.com
* **Corresponding author: Xiaogang Yin,** College of Chemistry and Materials Science, Guizhou Normal University, Guiyang, 550025, China, e-mail: m13885115516@163.com
Xiaokai Wu: College of Chemistry and Materials Science, Guizhou Normal University, Guiyang, 550025, China; R&D Department, Guizhou Material Industrial Technology Institute, Guiyang, 550014, China
Dingbo Shu, **Shengnan Huang:** College of Chemistry and Materials Science, Guizhou Normal University, Guiyang, 550025, China
Shaowen Huang: R&D Department, Guizhou Material Industrial Technology Institute, Guiyang, 550014, China; College of Materials and Metallurgy, Guizhou University, Guiyang, 550025, China
Chunping Yang: Guizhou Academy of Testing and Analysis, Guiyang, 550014, China
Bo Li: R&D Department, Guizhou Material Industrial Technology Institute, Guiyang, 550014, China

also possesses good mechanical properties that allow for easy processing (6,7). Unfortunately, the limited use of PBAT in the packaging industry is attributed to its low barrier properties, crystallization rate, and tensile strength (8). Therefore, a key strategy for future green development in the field of food preservation packaging is to modify PBAT materials to confer antimicrobial and antioxidant capabilities, as well as to improve their mechanical properties so that they can meet the application requirements of fruit and vegetable cling film.

This study aims to produce multifunctional biodegradable polyester cling film with antioxidant, antimicrobial, and barrier properties. Previous research has primarily focused on different nanoparticle composites, such as porous carbon nanoparticles (CNPs), TiO_2 nanoparticles, silver oxide (Ag_2O), and $ZnSnO_3$, which has shown that PBAT composites possess outstanding antibacterial and barrier properties (9–13). The research created bio-based nanocomposites based on Ag_2O and PBAT using the composite film casting process. These PBAT nanocomposite coatings exhibit superior mechanical, barrier, and antibacterial qualities, as well as excellent thermal stability (14). Electron microscopy also demonstrated the uniform distribution of Ag_2O throughout the PBAT matrix. However, these costly nanoparticles, which are potentially migratory packets of metal or metal oxide, pose a threat to human health and the environment when exposed. With phenolic hydroxyl groups giving them strong antioxidant and antimicrobial properties, films based on natural antioxidants, such as curcumin (CUR), tea polyphenols (TP), essential oils, and their complexes, are now a highly sought-after alternative to lower the harmful effects of chemical additives and nanoparticles on humans (15–17). For instance, researchers mixed polylactic acid (PLA), PBAT, and starch with cinnamyl aldehyde or TP to create antibacterial packaging (18). The outcomes demonstrated that the PLA/PBAT composite membrane could successfully inhibit the growth of *Staphylococcus aureus* and *Escherichia coli* at 4°C. Researchers compounded Aralia continentalis Kitagawa root extract (ARE) with chitosan (CH) to make composite packaging films, and the results showed that when the ARE content in the film was increased from 0.05 to 0.15 $mg{\cdot}mL^{-1}$, the high antioxidant capacity of the CH/ARE film was obtained (the DPPH and $ABTS^+$ free radical scavenging rate was increased) (19).

Research has been conducted on the antibacterial and antioxidant characteristics of PBAT and oregano-oil (OEO) antibacterial membranes for the storage of fish fillets. Researchers found that the inclusion of OEO can successfully impede the growth of *S. aureus* and *E. coli* (20). A wide variety of plants contain a family of naturally occurring active compounds known as plant polyphenols. Plant polyphenols, which possess a polyphenolic structure, exhibit high reducing abilities, scavenge free radicals, and shield biological macromolecules from free radical damage. They possess outstanding anti-inflammatory, antiviral, antibacterial, anti-aging, antioxidant, and preservation properties. Currently, they are extensively used to store and preserve fruits and vegetables, meat from cattle and poultry, and aquatic products, potentially enhancing the preservation effect and extending the shelf life. The plant polyphenol CUR has antibacterial, anti-inflammatory, anti-cancer, anti-aging, and anti-insulin properties. The rhizome of turmeric, which yields CUR, is commonly known as the "golden spice" due to its vivid yellow hue and adaptability. Its methoxy and hydroxy derivatives directly link to its antibacterial properties (21,22).

CUR, on the other hand, is incompatible with hydrophobic PBAT polymer materials due to its abundance of hydrophilic phenolic hydroxyl groups; when added alone, it is unable to diffuse homogenously within the PBAT matrix. Furthermore, when combined directly with the PBAT polyester material, CUR's high concentration of benzene rings, which are more rigid, may further impair the performance of the PBAT polymer. Additionally, maleic anhydride (SMA) is widely used in a variety of industries, including biomedical materials, water treatment agents, dispersants, viscosity reducers, and separation membranes. SMA offers benefits such as heat resistance, multiple reaction sites, high reactivity, and a nucleating agent effect (23–28). The maleic anhydride groups of SMA react readily with amino and hydroxyl groups. A base can neutralize the simultaneous production of anhydride and carboxyl groups from a carboxyl salt, which imparts water solubility to the polymer.

This study will graft and combine PBAT with maleic anhydride and CUR, leveraging the carboxylate nucleating agent role of maleic anhydride, its excellent compatibility with polyester materials, and the antibacterial and antioxidant advantages of CUR. This process naturally enhances the compatibility between CUR and PBAT polyester materials, leading to improved mechanical properties, processing performance, and the dispersion of CUR with PBAT polyester. With promising market prospects, this approach meets both environmental protection and practical application requirements, aligning with existing policy guidelines and consumer demand.

The primary goal of this study is to prepare PBAT/CUR−SMA composite packaging film that possesses strong antibacterial activity, antioxidant qualities, and good mechanical properties for use in food packaging applications. Grafting CUR onto SMA yielded the CUR−SMA modifier and film blowing and extrusion methods were used to produce the PBAT/CUR−SMA composite film. The objectives include achieving better dispersion of CUR in PBAT polyester, enhancing the antimicrobial and antioxidant properties of the PBAT composite film, and improving the

processing and molding properties, tensile strength, and gas barrier of the PBAT material. This work meticulously examined the structural, barrier, antibacterial, antioxidant, mechanical, and packaging freshness retention qualities of the PBAT composite films to determine how the addition of CUR–SMA affected them.

2 Experimental

2.1 Materials

PBAT was purchased from The Xinjiang Lanshan Hetun Polyester Co. CUR, with 95% purity, was supplied by Angi Chemicals Ltd. The styrene–maleic anhydride copolymer, with styrene abbreviated as S and maleic anhydride as MA in a ratio of S:MA = 1:1, was obtained from Cleverly (model SMA1000). 4-Dimethylaminopyridine (DMAP), with 97% purity, was obtained from Aladdin's Reagent Ltd. 1,4-Dioxane, with 97% purity, was obtained from Macklin. Sodium hydroxide, with 97% purity, and petroleum ether, with 97% purity, were obtained from Macklin. The bacteria used in the antibacterial test is *S. aureus* ATCC6538 and was supplied by Guangdong Microbial Culture Collection Center (GDMCC). Porcine pancreatic lipase, with 15–35 units/mg, and phosphate buffer solution, with pH 7.2 were obtained from Macklin.

2.2 Preparation of CUR–SMA

About 26 g of maleic anhydride (SMA) is taken in a 500 mL round-bottomed flask. A total of 200 mL of 1,4-dioxane is added as a solvent, and SMA is dissolved at 60°C with stirring. Then, 36 g of CUR, 7.2 g of sodium hydroxide, and 1.5 g of DMAP are added, and the reaction is stopped after stirring for 4 h at 60°C. After cooling to room temperature, the product is poured into a large amount of petroleum ether to precipitate the solid product, filtered, and washed with distilled water to obtain the solid product, which is then dried in an oven at 60°C until it reaches a constant weight. The solid yields are ground to obtain a powdered solid product, CUR–SMA.

2.3 Preparation of PBAT/CUR–SMA films

PBAT/CUR–SMA composites are prepared using the extrusion blown film technique. PBAT microspheres are first dried at 80°C. PBAT/CUR–SMA composites with different ratios (0.1 wt%, 0.3 wt%, 0.5 wt%, 0.7 wt%, and 0.9 wt%) are prepared using a twin-screw extruder, and the 0.5 wt% CUR/PBAT composite serves as a control. From the feed zone (1) to the mold zone (5), the barrel temperatures are set at 105°C, 135°C, 145°C, 150°C, and 155°C and the screw speed is 180 rpm·min^{-1}. After extrusion is completed, granulation and drying are carried out. PBAT/CUR–SMA composite films with different contents of CUR–SMA are prepared using a single screw film blowing machine. A 0.5 wt% CUR/PBAT composite membrane with pure PBAT serves as a control. From the feed zone (1) to the mold zone (5), the temperature distribution of the screw is 110°C, 130°C, 135°C, 140°C, and 145°C with a speed of 700 rpm·min^{-1}. The products are named as PBAT, PBAT/0.5% CUR, PBAT/0.1% CUR–SMA, PBAT/0.3% CUR–SMA, PBAT/0.5% CUR–SMA, PBAT/0.7% CUR –SMA, and PBAT/0.9% CUR–SMA.

2.4 Characterization

2.4.1 Fourier transform infrared (FTIR) spectroscopy

All materials were subjected to infrared spectroscopic analysis using an ATR-FTIR device (model Nicolet ARE50). This equipment is designed to capture FTIR spectra of samples in the wavenumber range from 4,000 to 500 cm^{-1}.

2.4.2 ^{1}H NMR spectra of CUR–SMA

The ^{1}H NMR spectra of the sample solutions were acquired using a Bruker Avance NEO 400 MHz NMR spectrometer. Specifically, 10 mg of CUR and 10 mg of SMA were each dissolved in deuterated chloroform ($CDCl_3$), while 10 mg of the CUR–SMA complex was dissolved in a mixture of deuterated methanol (CD_3OD) and deuterated chloroform.

2.4.3 Thermogravimetric analysis and calculation of the graft degree of CUR

The thermogravimetric analysis was conducted using a TGA-DTG thermogravimetric analyzer (model TGAQ50). All measurements were performed under a continuous flow of nitrogen. The temperature range was from ambient to 600°C, with a heating rate of 10°C·min^{-1}.

2.4.4 Assay of antibacterial activity

The antibacterial inhibition test of the CUR–SMA bacteriostatic modifier was conducted using the zone of inhibition

method. A 10 mg·mL^{-1} sample was diluted tenfold and mixed with agar medium to create a suspension containing 108 CFU·mL^{-1}. The samples were incubated at 37°C for 24 h. The antibacterial effect was determined by examining the formation and dimensions of the inhibition zones. For the *in vitro* testing of PBAT/CUR−SMA composite membranes, a similar procedure was followed. However, the samples were molded into circular membranes with a diameter of 23 mm. Additionally, the concentration of the bacterial suspension was adjusted to 104 CFU·mL^{-1}. The inhibition zones' diameters were measured using a ruler, and the inhibitory effect was assessed based on the size of these zones.

2.4.5 Antioxidant activity of the films

The antioxidant activity of PBAT/CUR−SMA composite membranes is assessed using the DPPH method. Initially, the film samples are cut into small pieces (0.1 g) and then mixed with 5 mL of a methanol solution. The mixture is sonicated for 20 min, left to stand at room temperature for 10 h, and subsequently centrifuged at 5,000 r·min^{-1} for 10 min. Post-centrifugation, 1 mL of the supernatant is combined with 3 mL of 0.12 mmol·L^{-1} DPPH methanol solution and allowed to react for 1 h at room temperature. A blank control is prepared by mixing 1 mL of methanol solution with 3 mL of DPPH solution. The DPPH radical scavenging activity is determined using the following equation (20):

$$\text{Radical scavenging activity (\%)} = \frac{1 - A_{\text{sample(517nm)}}}{A_{\text{blank control(517nm)}}} \times 100\%, \quad (1)$$

where A_{sample} is the absorbance of the sample and $A_{\text{blank control}}$ is the absorbance of the blank sample (DPPH solution).

2.4.6 Crystallization properties

The crystallization characteristics of the composite were examined using differential scanning calorimetry (DSC25, TA Instruments, USA). Each sample was analyzed under a nitrogen gas purge, with an empty crucible serving as the reference. The testing protocol involved rapidly heating the sample to 250°C at a rate of 10°C·min^{-1} and maintaining it at that temperature for 2 min to eliminate any residual thermal history. Following this, the sample was cooled from 250°C to 25°C at the same rate of 10°C·min^{-1}. Then, the temperature was increased back to 250°C at the same rate. Throughout this process, the relationship between the heat flow and temperature was meticulously recorded. Using Eq. 2, the degree of crystallinity of the sample is calculated:

$$X_c = \frac{\Delta H_m}{(1 - \varphi)\Delta H_m^0} \times 100\% \quad (2)$$

where X_c, ΔH_m, and ΔH_m^0 are the degree of crystallinity (%), the enthalpy of melting (J·g^{-1}), and the enthalpy of melting at 100% crystallization of PBAT (114 J·g^{-1}), respectively (29), and $1 - \varphi$ is the mass fraction of PBAT in the composite.

2.4.7 Mechanical properties of the PBAT/CUR−SMA composite films

The longitudinal tensile strength, transverse tensile strength, longitudinal elongation at break, and transverse elongation at break for PBAT and PBAT/CUR−SMA were determined using a microcomputer-controlled electronic universal testing machine (SNAS, CMT6104). The film samples were cut into dumbbell shapes, both longitudinally and transversely, and tested at room temperature with a tensile speed of 200 mm·min^{-1}. Each sample was subjected to at least five parallel tests, and the results were averaged to minimize errors.

2.4.8 Water vapor transmission rate

The water vapor barrier properties of laminated films were assessed in accordance with the standard CB1037-88, using a Labthink C360M Water Vapor Transmission Rate Tester. The experiments were conducted employing the weight loss technique at a constant temperature of 38°C and a relative humidity of 10%. Samples of PBAT/CUR−SMA laminated films, varying in their composition of pure PBAT and CUR−SMA, were positioned within a permeable filled with 10 mL of mineral water (with a test area of 32.95 cm^2). This setup was used to determine the water vapor permeability rate (WVP) of the laminated films.

2.4.9 Oxygen barrier properties

The oxygen barrier properties of the composite films were assessed using an oxygen transmission tester. This equipment was imported from MOCON, Denmark (model specification OX-TRAN2/12). The tests were conducted at a temperature of 23°C over an area of 50 cm^2.

2.4.10 Water contact angle

The hydrophobicity of the composite films was evaluated using an angular measuring instrument manufactured by Kruse GmbH (Germany, specification number DSA25).

2.4.11 Scanning electron microscopy (SEM)

A scanning electron microscope (Zeiss, Germany, Gemini SEM 360) was used to observe the fracture morphology of the film after sputtering with gold plating at a magnification of 10,000 times.

2.4.12 BET surface area

The specific surface area of the composite films was evaluated using a fully automated specific surface area and porosity meter (Kantar Corporation, USA, model NOVA-1000e).

2.4.13 Biodegradation test

The PBAT/CUR−SMA composite membrane was prepared into small squares of 2 cm × 2 cm and placed in 0.6% porcine pancreatic lipase phosphate buffer. Three sets of parallel experiments were set up for each group of membranes, which were continuously oscillated using the electrothermal thermostatic oscillating water tank (Shanghai Yihang Scientific Instrument Co. Ltd.) with the temperature set at 40°C. Samples were taken every 5 days and weighed; the quality change was recorded, and the enzyme solution was replaced. Changes in the surface of the membrane were photographed and recorded (30).

2.4.14 Food packaging applications

To assess the application of PBAT/CUR−SMA in food packaging, perishable fruits (strawberries, apples) and vegetables (oyster mushrooms) are selected. Fresh strawberries, flat mushrooms, and cut apples are packaged with PBAT/0.5% CUR−SMA and PBAT/0.9% CUR−SMA, respectively, with plain PBAT film serving as a control. The fresh apples are washed, dried, peeled, cut into round and thin slices, divided into three groups like strawberries, and kept at 15°C for 5 days. The weight of the sample and the daily change of the sample were recorded. The weight loss was calculated using the following equation (31):

$$\text{Weight loss}(\%) = \frac{W_1 - W_2}{W_1} \times 100\% \quad (3)$$

where W_1 and W_2 are the weights of the samples before and after the different storage stages, respectively.

2.4.15 Statistical analysis

The data are expressed as mean ± standard deviation. Statistical significance among the datasets was assessed using ANOVA via SPSS 21(IBM, New York, USA). Post hoc comparisons of mean values were determined using Tukey's multiple range tests at a 5% significance level (32).

3 Results and discussion

3.1 CUR−SMA structural characterization

The grafting principle of CUR and SMA is illustrated in Figure 1(a). As observed in Figure 1(b), an absorption peak at 3,410 cm^{-1}, attributed to the stretching vibration of the phenolic hydroxyl group of CUR, is present in the CUR+SMA spectrum (33). The absorption peaks at 1,780 and 1,857 cm^{-1} are typical characteristic absorption peaks of acid anhydride (34). In the infrared spectrum of CUR−SMA, a noticeable weakening of the anhydride group's absorption is evident, which may be attributed to a small proportion of the anhydride group that has not undergone ring-opening. Additionally, the ester bond absorption peak at 1,712 cm^{-1} is significantly intensified, confirming the successful grafting of SMA onto CUR.

The NMR hydrogen spectra of CUR, SMA, and CUR−SMA are depicted in Figure 1(c). CUR exhibits proton peaks corresponding to the phenolic hydroxyl group at δ = 5.80 ppm, to the olefinic protons at δ = 6.48 and 6.94 ppm, and to the aromatic protons on the benzene ring at δ = 7.05, 7.12, and 7.59 ppm. The NMR spectra of the CUR−SMA reveal a weakening and a high-field shift of the proton peaks associated with the phenolic hydroxyl group. This indicates that the grafting of the phenolic hydroxyl group with the ring-opening anhydride group has been successfully achieved. The strong electron-withdrawing effect of the anhydride group's carbonyl (C═O) moiety results in a reduction of proton-electron density within the CUR molecule, enhancing the de-shielding effect and causing a shift to a lower magnetic field, which is reflected in a larger chemical shift.

3.2 Thermal stability and the graft degree of CUR

The thermal behaviors of CUR, SMA, and CUR+SMA are analyzed using TGA and DTG. The thermogravimetric diagram (Figure 2a) reveals that the CUR+SMA sample has two weight loss stages. The initial stage occurs between 73°C and 195°C characterized by a 6.4% weight loss attributed to the evaporation of moisture within the sample. Due to the

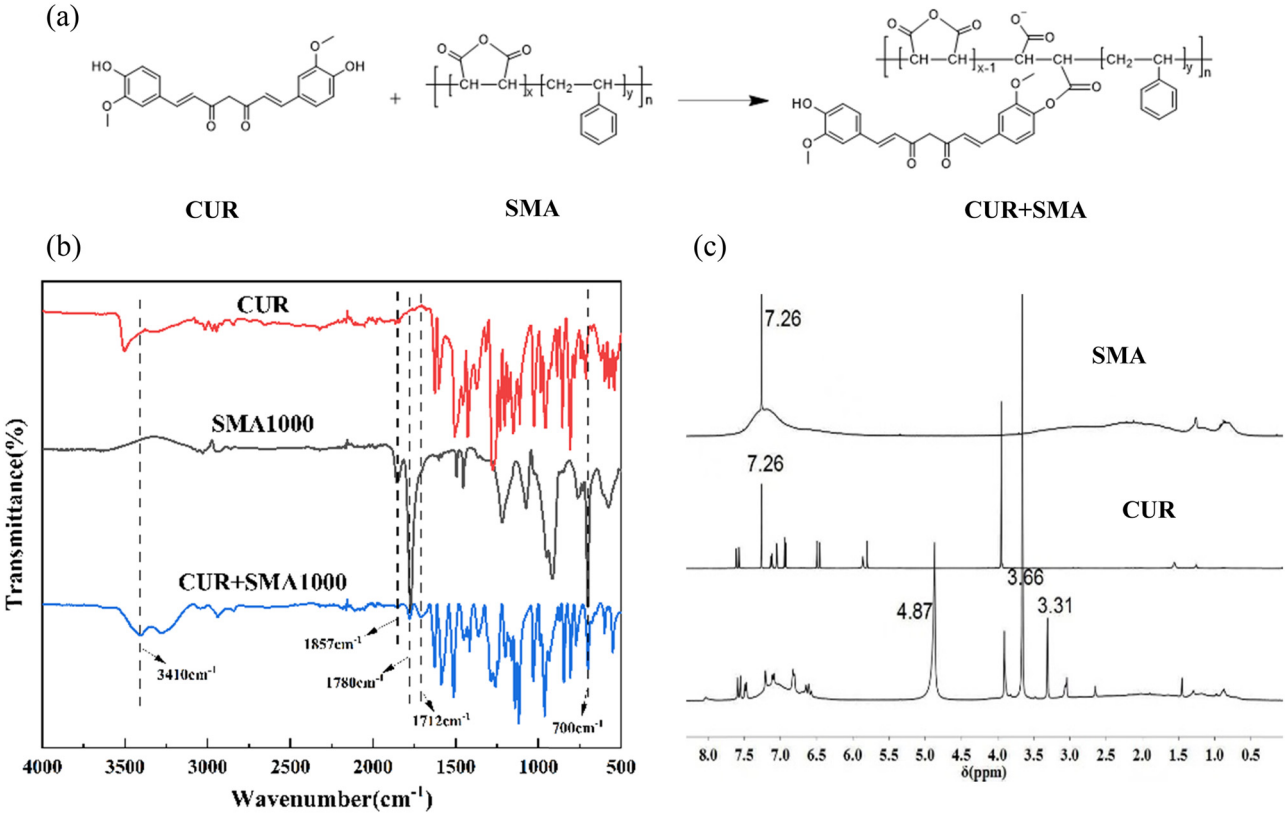

Figure 1: (a) Response principle of CUR and SMA. (b) FT-IR spectra of CUR, SMA, and CUR+SMA. (c) 1H NMR spectra of SMA, CUR, and CUR–SMA.

formation of new chemical bonds, the second stage occurs between 225°C and 423°C and is marked by a significant weight loss of 59.45%. Due to the breakdown of the chemical bonds in the sample, the weightlessness phase of CUR occurred between 272°C and 424°C, and that of SMA occurred between 274°C and 473°C.

As the temperature increases, the chemical bonds break, leading to a new stage of weight loss. Figure 2b (DTG) displays the temperature at which the sample decomposes at its maximum rate. The maximum decomposition rate of CUR occurs at 382°C, and those of SMA and CUR+SMA occur at 388°C and 372°C, respectively. The results indicate

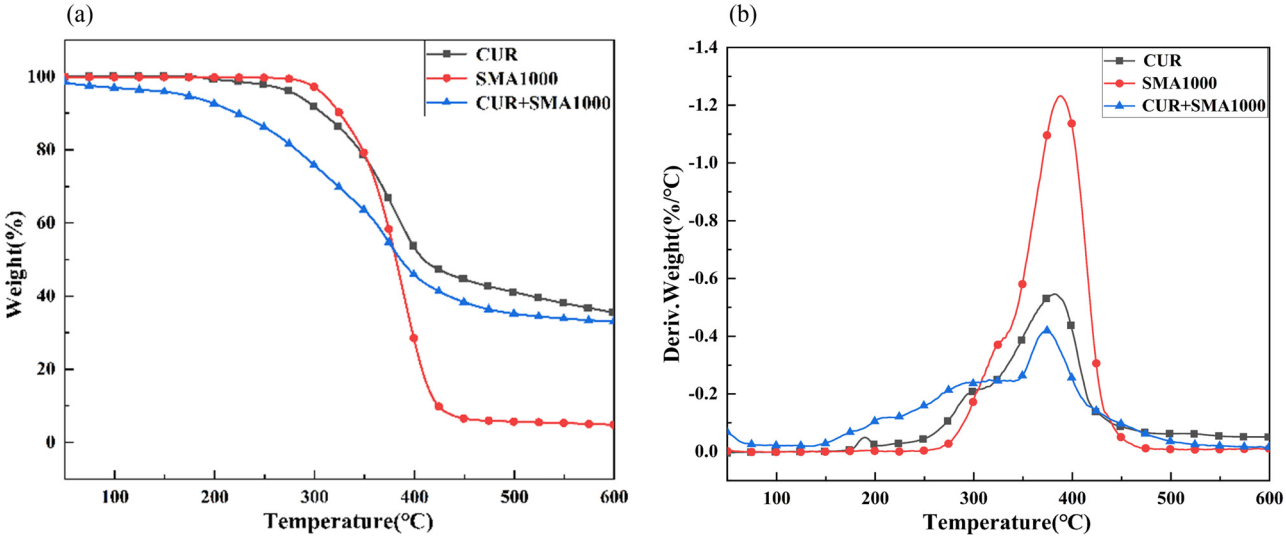

Figure 2: (a) TG curves and (b) DTG curves of CUR, SMA, and CUR+SMA.

that the thermal stability of CUR+SMA is lower than that of the other two materials, which is advantageous in certain applications.

Calculating the graft degree of CUR, as shown in Figure 2(a), the weight losses of CUR, SMA1000, and CUR+SMA1000 are basically unchanged at 600°C and are 35.54%, 4.80%, and 32.99%, respectively. Assuming that CUR has a mass of X grams and SMA1000 has a mass of Y grams, the graft degree can be determined by using the law of conservation of mass:

$$(1 - 35.54\%)X + (1 - 4.80\%)Y = (X + Y)(1 - 32.99\%).$$

The graft degree of CUR is CUR/SMA1000 = X/Y = 11.05.

3.3 Antibacterial performance analysis

There are diverse antibacterial agents, and some of them have significant effects on *E. coli*, *S. aureus*, etc. (35). The present study shows that CUR exerts its antibacterial action primarily by causing depolarization of the bacterial cell membrane, dismantling the structural integrity of the bacterial cell membrane, and disrupting the normal metabolic processes of bacteria, thereby achieving its antibacterial impact (36). To evaluate the antibacterial properties of CUR–SMA, we conducted experiments on *S. aureus*. The results are shown in Figure 3 and Table 1. Studies have shown that SMA has no antibacterial effect on *S. aureus*, while pure CUR has an obvious antibacterial effect on *S. aureus*. The antibacterial effect of the PBAT/CUR–SMA composite membrane on *S. aureus* first increased and then decreased with the addition of CUR, which proved that the modified PBAT/CUR–SMA composite membrane retained the antibacterial properties of CUR. Adding CUR–SMA to the antibacterial food packaging film could reduce the spoilage rate of fruits and vegetables and expand the application range of PBAT.

3.4 DPPH-radical scavenging activity

Packaging films that incorporate antioxidants can prevent product deterioration and extend shelf life by neutralizing reactive oxygen species within the packaging system (37). DPPH tests are frequently employed to evaluate the antioxidant capacity. In this study, the CUR-SMA modifier, predominantly composed of CUR, exhibits antioxidant

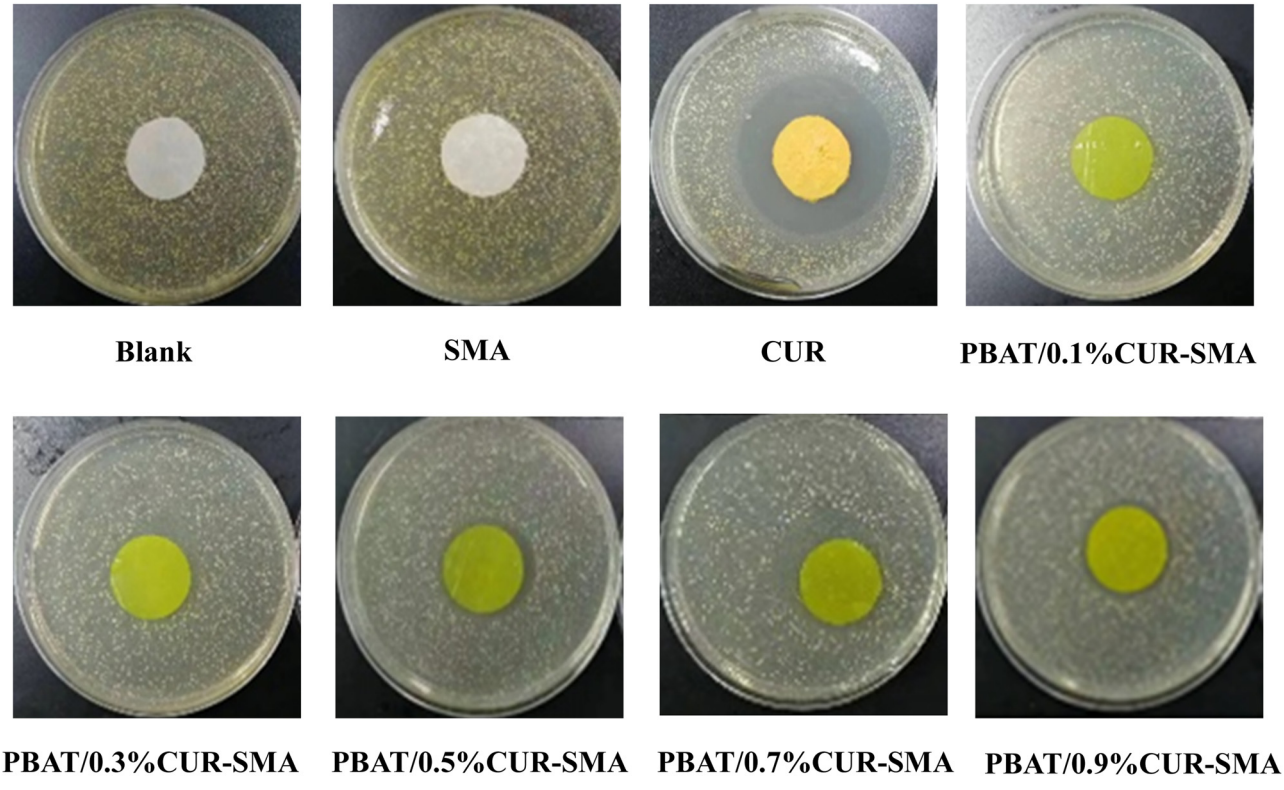

Figure 3: The antibacterial activity of the PBAT/CUR–SMA composite membrane with SMA and CUR, and different concentrations of CUR–SMA modifier are detected against *S. aureus*.

Table 1: Results of antibacterial activity of the resulting PBAT-based films

Sample	Diameter of the bacterial growth inhibition zone (mm)
Blank	0
SMA	0
CUR	65
PBAT/0.1%CUR–SMA	24
PBAT/0.3%CUR–SMA	27
PBAT/0.5%CUR–SMA	30
PBAT/0.7%CUR–SMA	33
PBAT/0.9%CUR–SMA	25

properties attributed to its two phenolic hydroxyl groups. Antioxidant-active PBAT/CUR–SMA composite films are prepared by adding different concentrations of CUR–SMA to PBAT. The linear relationship between antioxidant capacity and CUR–SMA concentration is shown in Figure 4. The antioxidant capacity of the composite film is determined by measuring the absorbance of DPPH˙ at 517 nm (38). The addition of CUR–SMA enhanced the antioxidant activity of the PBAT/CUR–SMA composite film compared to the DPPH methanol solution control. The antioxidant activity is enhanced with increasing CUR–SMA content. The absorbance of the PBAT/CUR–SMA composite film decreased from 0.93 to 0.26, and the free radical scavenging capacity increased from 2.73% to 72.26%. The findings demonstrate that the PBAT/CUR–SMA composite film possesses substantial antioxidant activity, rendering it a viable candidate for application in packaging film.

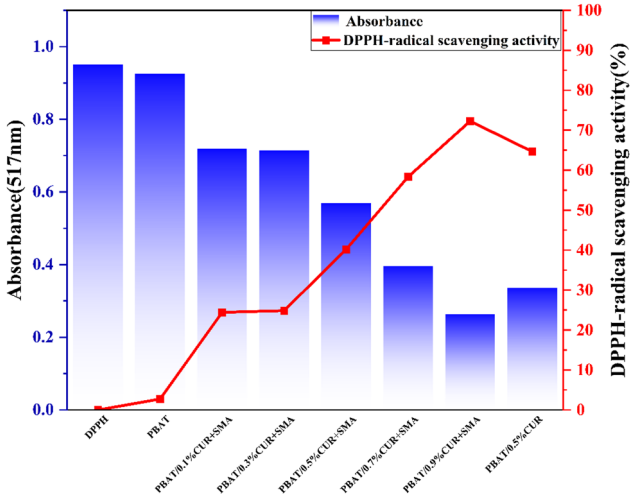

Figure 4: Absorbance and free radical scavenging activity of the PBAT/CUR–SMA composite films.

3.5 Non-isothermal crystallization behavior of composite films

DSC is a technique that reveals the relationship between physical or chemical changes and thermal effects (39). Figure 5(a) and (b) shows the DSC curves for the second heating and first cooling of the PBAT/CUR–SMA composite film. The crystallization temperature (T_c), enthalpy of crystallization (ΔH_c), melting temperature (T_m), enthalpy of melting (ΔH_m), and degree of crystallinity (X_c) associated with the composites are shown in Table 2. The crystallization

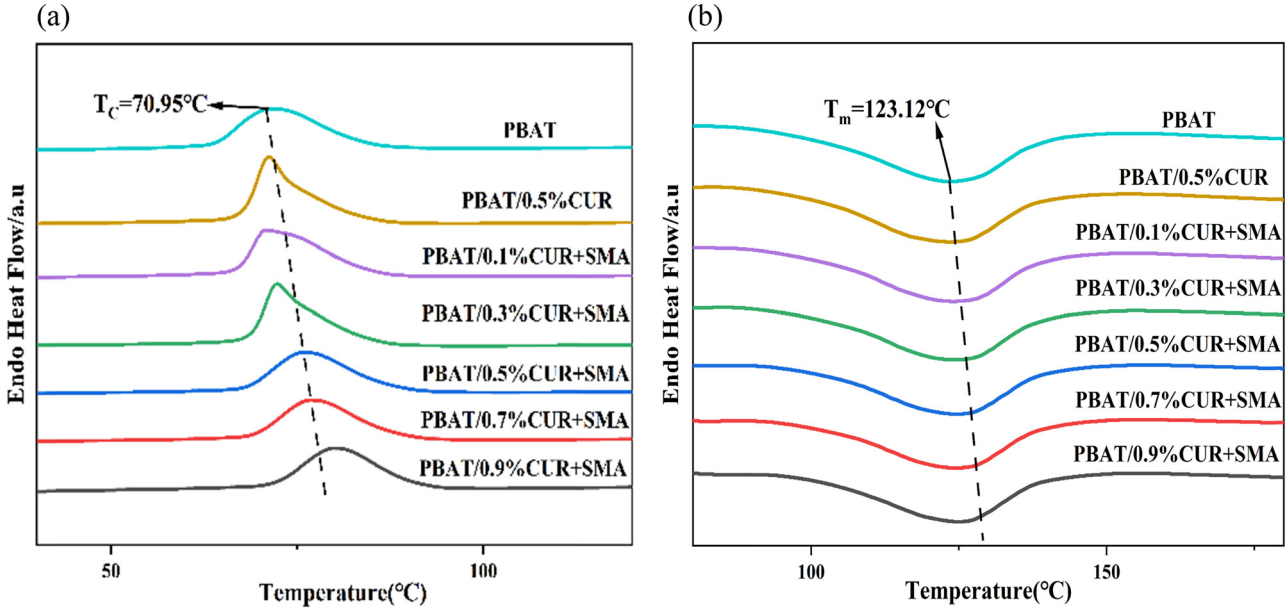

Figure 5: (a) First cooling process and (b) the second heating process of the PBAT/CUR–SMA composite.

Table 2: Crystallization properties of the composite materials

Samples	T_C (°C)	ΔH_C (J·g^{-1})	T_m (°C)	ΔH_m (J·g^{-1})	X_C (%)
PBAT	70.95	18.91	123.12	12.66	11.11
PBAT/0.5%CUR	71.59	17.27	123.20	13.29	11.72
PBAT/0.1%CUR–SMA	71.77	16.78	123.48	12.56	11.03
PBAT/0.3%CUR–SMA	72.32	17.24	124.15	12.42	10.93
PBAT/0.5%CUR–SMA	76.01	16.11	124.56	11.60	10.23
PBAT/0.7%CUR–SMA	76.83	16.13	124.72	8.60	7.60
PBAT/0.9%CUR–SMA	79.98	15.67	125.31	7.82	6.92

temperature (T_c), enthalpy of crystallization (ΔH_c), melting temperature (T_m), enthalpy of melting (ΔH_m), and degree of crystallinity (X_c) associated with the composites are shown in Table 2. The variation of the crystallization profile during the first cooling of the composites is shown in Figure 5(a). As observed from Table 2, the T_C of the PBAT/CUR–SMA composites increased from 71.77°C to 79.98°C and ΔH_C decreased from 18.91 to 15.67 J·g^{-1} compared to those of pure PBAT. These changes are due to the heterogeneous nucleation of CUR, which is facilitated by the addition of SMA. This addition improves the dispersion effect of CUR in PBAT and enhances the compatibility of CUR with PBAT. The ΔH_m of the composites also decreased from 12.66 to 7.82 J·g^{-1} with the incorporation of SMA.

The CUR–SMA modifier increased the T_m of the composites. A decrease in ΔH_m is advantageous for the processing of these composites, as a smaller ΔH_m indicates that less heat is required for processing. The incorporation of CUR–SMA modifier reduced the crystallinity (X_c) of the composites, which is attributed to the fact that the incorporation of the modifier containing CUR–SMA reacted with PBAT to form a branching structure and an entangled network structure, which restricted the movement of the PBAT molecular chains and impeded the orderly arrangement of the molecules, leading to a decrease in crystallinity (40).

3.6 Characterization of mechanical properties of the composite films

The variations in the mechanical properties of the PBAT/CUR–SMA composite film are shown in Figure 6(a) and (b) and Table 3. As the CUR–SMA content in the PBAT matrix increased from 0.1 wt% to 0.9 wt%, both the tensile strength and elongation at break first increased and then decreased. Compared with PBAT and PBAT/0.5% CUR, the tensile

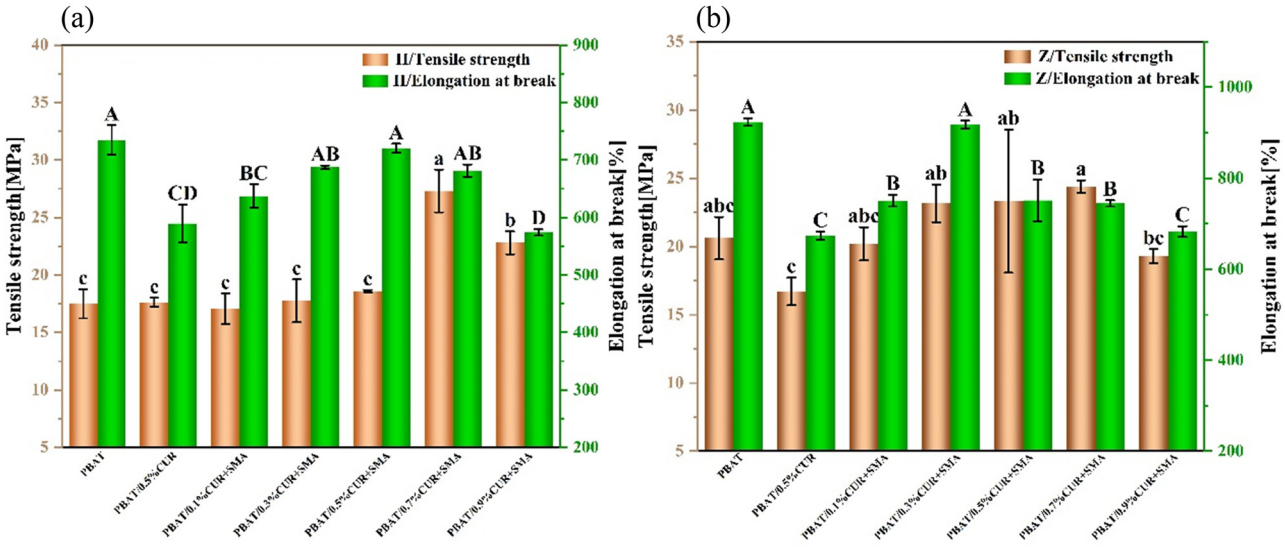

Figure 6: (a) Transverse, (b) longitudinal tensile strength, and elongation at break of PBAT and its composite films. Different letters within the same indicator indicate significant differences among the film samples at $P < 0.05$.

Table 3: Mechanical properties of the PBAT/CUR–SMA composite films

Samples	Tensile strength (MPa)		Elongation at break (%)	
	Longitudinal	Transverse	Longitudinal	Transverse
PBAT	20.6	17.5	923.5	734.8
PBAT/0.5%CUR	16.7	17.6	673.1	589.5
PBAT/0.1%CUR–SMA	20.2	17.1	750.7	637.2
PBAT/0.3%CUR–SMA	23.1	17.8	918.0	687.4
PBAT/0.5%CUR–SMA	23.3	18.6	750.9	720.6
PBAT/0.7%CUR–SMA	24.4	27.3	744.6	681.4
PBAT/0.9%CUR–SMA	19.3	22.8	682.7	574.1

strength of the PBAT/0.7% CUR–SMA composite film is significantly enhanced, and the mechanical properties of the CUR–SMA composite film are significantly improved. This improvement is attributed to the anhydride functional groups in the modifier, which are capable of undergoing chain extension reactions with the terminal hydroxyl or carboxyl groups of the PBAT polyester material, thereby enhancing the inherent properties of the PBAT polyester.

Concurrently, the improved interfacial compatibility is the primary reason for the improved mechanical properties of the film, as the maleic anhydride copolymer itself is extremely compatible with the PBAT polyester material (4). However, when CUR–SMA is added in excess, agglomeration and excessive cross-linking reactions between the two molecules occur in the composite film matrix, resulting in a decrease in the tensile strength and elongation at break of the composite film (41).

3.7 Water vapor barrier properties

Water vapor permeability (WVP) is a critical property when selecting packaging materials. The water vapor barrier performance of the PBAT/CUR–SMA composite film was tested by a water vapor permeability tester, and the results are shown in Table 4 and Figure 7. The WVP of pure PBAT is the highest; however, the addition of a CUR–SMA modifier to the PBAT/CUR–SMA composite film resulted in a decrease in WVP. Specifically, PBAT/0.5% CUR–SMA has a 40% reduction in WVP compared to pure PBAT. The lower the WVP, the lower the water vapor permeability of the film, the better the barrier performance, and the more conducive to the long-term preservation of the product (42). This improvement is attributed to the formation of an intramolecular hydrogen bond between C═O on PBAT and OH on CUR–SMA and the transport of water molecules is hindered. Moreover, the anhydride functional groups in the modifier combine with the terminal hydroxyl or terminal carboxyl groups of the PBAT polyester material in a chain expansion reaction, resulting in a tighter polymer molecular chain. Therefore, the addition of CUR–SMA improves the air tightness of the composite film. These findings suggest that the PBAT/CUR

Table 4: Thickness and WVP of the PBAT/CUR–SMA composite films

Samples	Thickness (mm)	WVP (10^{-13} g·cm·cm^{-2}·S·Pa)
PBAT	0.027	2.61
PBAT/0.1%CUR+SMA	0.031	1.66
PBAT/0.3%CUR+SMA	0.024	1.56
PBAT/0.5%CUR+SMA	0.033	1.53
PBAT/0.7%CUR+SMA	0.029	2.22
PBAT/0.9%CUR+SMA	0.034	2.23

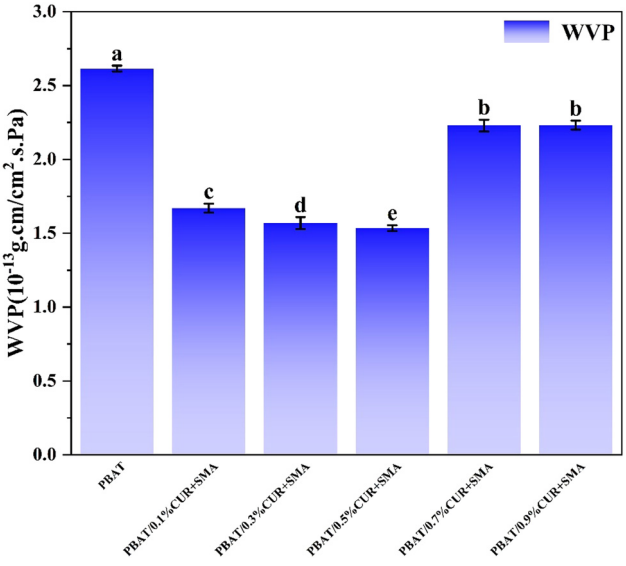

Figure 7: WVP for the PBAT/CUR–SMA laminated films. Different letters within the same indicator indicate significant differences among the film samples at $P < 0.05$.

Table 5: Thicknesses and oxygen barrier properties of the PBAT/CUR−SMA composite films

Samples	Thickness (mm)	Oxygen transmittance (cc/(m^2·day))
PBAT	0.42	27.11
PBAT/0.5%CUR	0.45	22.70
PBAT/0.1%CUR+SMA	0.38	29.69
PBAT/0.3%CUR+SMA	0.35	23.29
PBAT/0.5%CUR+SMA	0.33	15.98
PBAT/0.7%CUR+SMA	0.29	69.92
PBAT/0.9%CUR+SMA	0.26	62.93

−SMA composite film has potential applications in food packaging.

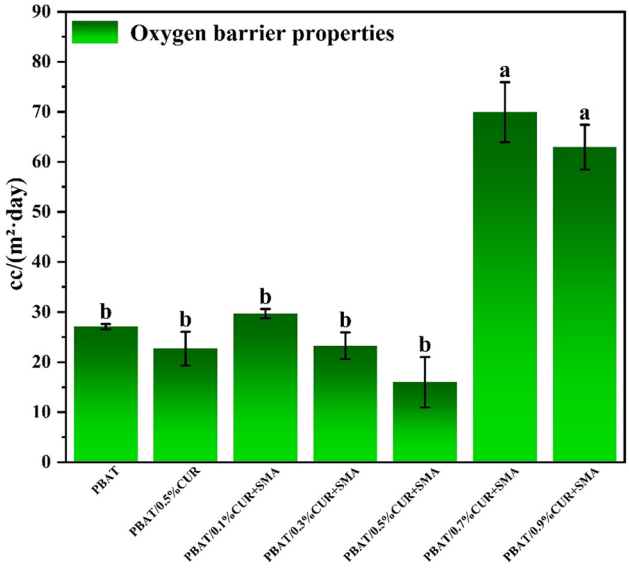

Figure 8: Oxygen barrier properties of the PBAT/CUR−SMA laminated films. Different letters within the same indicator indicate significant differences among the film samples at $P < 0.05$.

3.8 Oxygen barrier properties

Oxygen barrier properties are also central to assessing the effectiveness of a film's gas barrier and are important in determining the limitations of a film's use in packaging applications. The oxygen barrier properties of PBAT/CUR−SMA composite films were tested using an oxygen transmission rate tester. As shown in Table 5 and Figure 8, PBAT/0.5% CUR+SMA had the lowest oxygen transmission rate and the best oxygen barrier performance. The oxygen transmittance decreased from 22.33 to 15.98 cc·(m^2-day)$^{-1}$ with the addition of CUR−SMA to the PBAT matrix, which indicated that CUR−SMA played a role in improving the oxygen barrier performance of the films and enhancing the freshness retention of the films. However, the higher oxygen permeability of PBAT/0.7% CUR+SMA and PBAT/0.9% CUR+SMA composite films compared to those of PBAT could be attributed to the increase in the dosage of CUR−SMA and its poor compatibility with PBAT, which resulted in poorer oxygen barrier properties of the films.

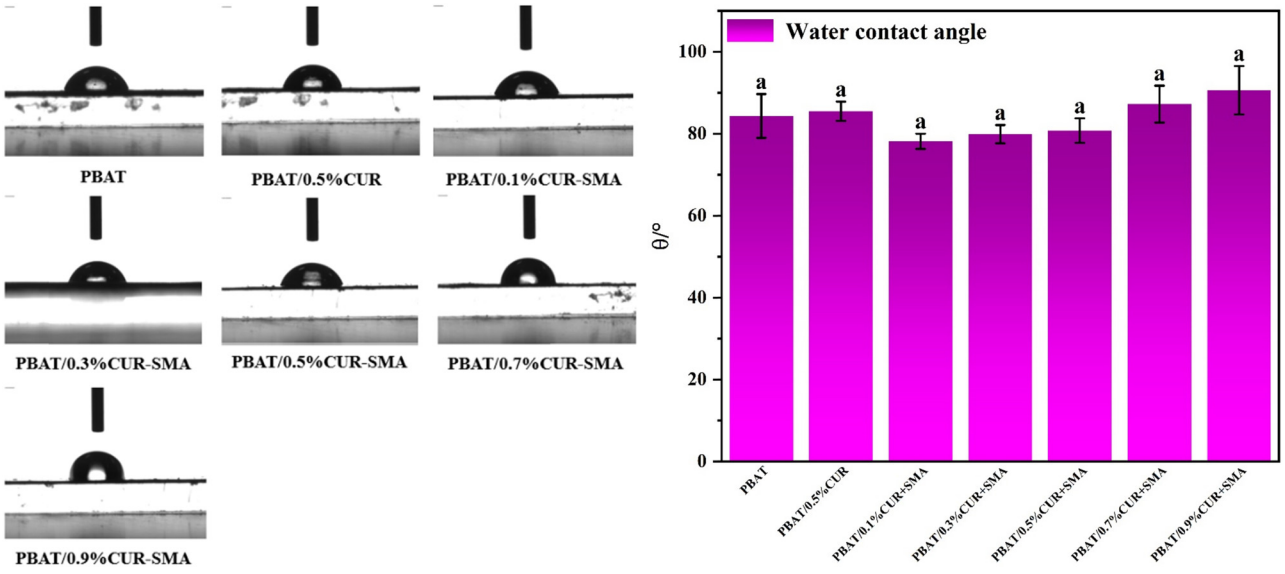

Figure 9: Water contact angles of the PBAT/CUR−SMA laminated films. Different letters within the same indicator indicate significant differences among the film samples at $P < 0.05$.

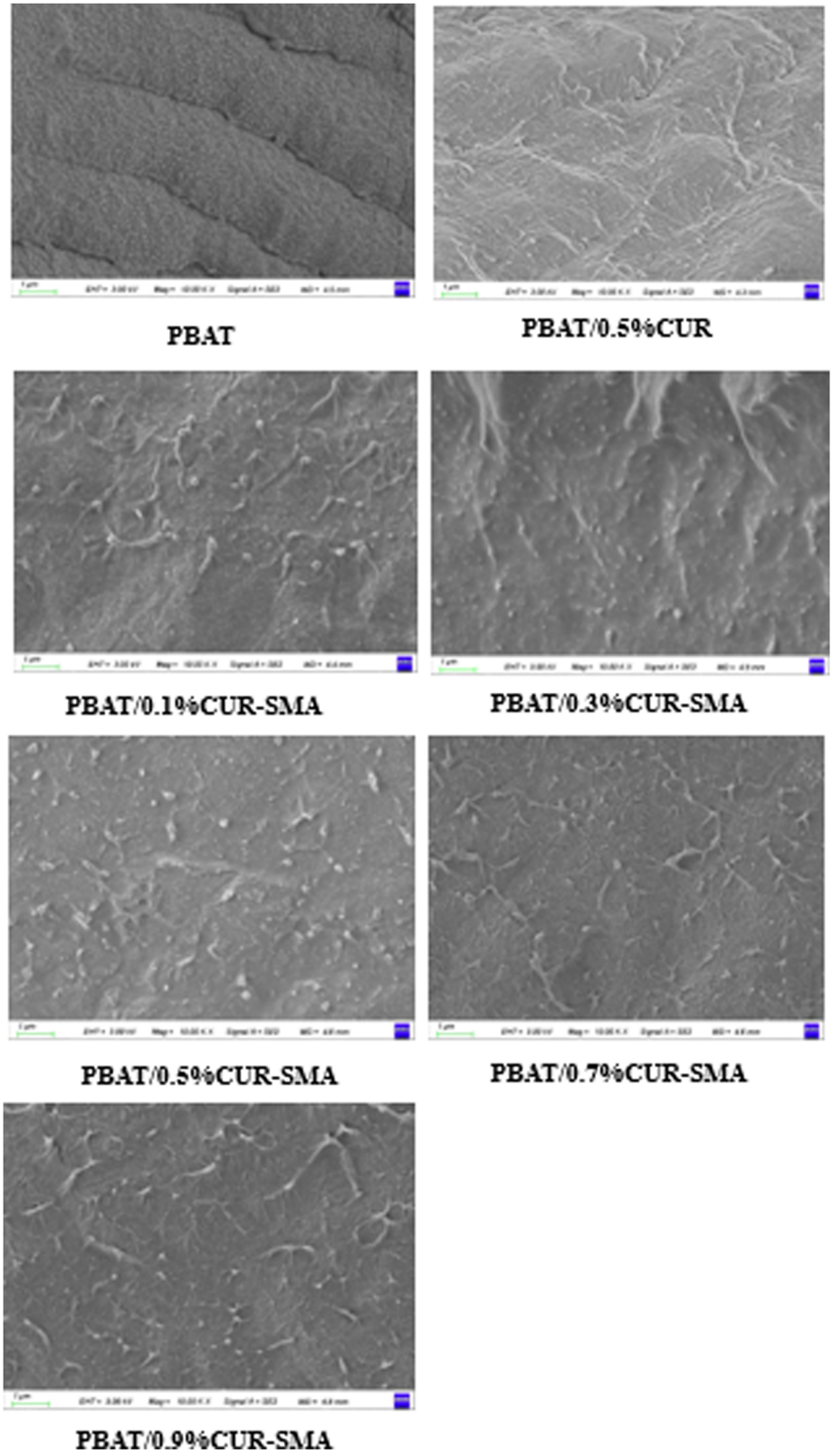

Figure 10: Fracture morphologies of the PBAT/CUR–SMA laminated films.

Table 6: Surface areas of the PBAT/CUR–SMA composite films

Samples	Weight (mg)	Surface area ($m^2 \cdot g^{-1}$)
PBAT	19.53	6.63
PBAT/0.5%CUR	17.25	8.18
PBAT/0.1%CUR+SMA	19.87	7.84
PBAT/0.3%CUR+SMA	24.76	4.24
PBAT/0.5%CUR+SMA	22.66	22.95
PBAT/0.7%CUR+SMA	23.87	4.77
PBAT/0.9%CUR+SMA	25.21	6.67

3.9 Water contact angles

The water contact angle is a measure of the hydrophilic or hydrophobic nature of a material. As shown in Figure 9, the water contact angle of the PBAT/0.1% CUR–SMA film is the smallest, which is attributed to the addition of the hydrophilic –OH group from CUR–SMA to PBAT, thereby making the composite film more hydrophilic. However, as the amount of CUR–SMA increases, a large number of –OH groups react with the –COOH groups in PBAT to form esters, which reduces the hydrophilicity of the composite film and increases its hydrophobicity.

3.10 Fracture morphology

As shown in Figure 10, the fracture surface of PBAT is relatively smooth. The PBAT/0.5% CUR film's fracture surfaces are not smooth, and the PBAT/0.1% CUR–SMA films have significantly fewer particles with uneven distribution and poor compatibility, resulting in poor mechanical properties. The fracture surfaces of the three composite films – PBAT/0.3% CUR–SMA, PBAT/0.5% CUR –SMA, and PBAT/0.7% CUR–SMA – exhibit less overall granularity and are more uniformly distributed, indicating better compatibility and improved mechanical properties. The PBAT/0.9% CUR–SMA composite films show severe agglomeration, strong granularity, poor compatibility, and poor mechanical properties.

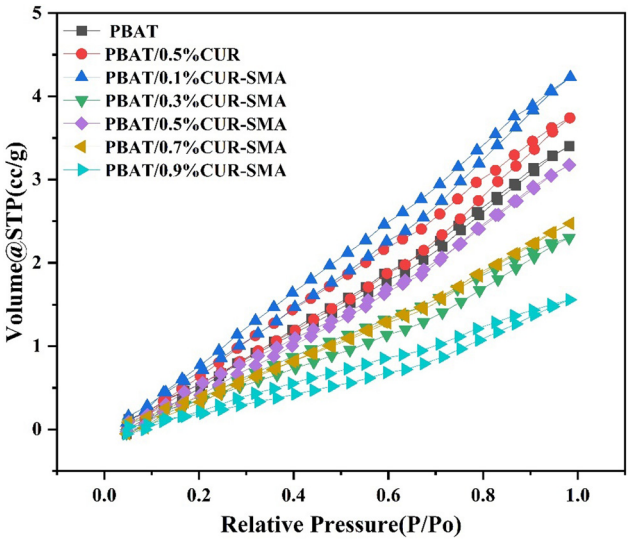

Figure 11: Volume@STP of the PBAT/CUR–SMA laminated films.

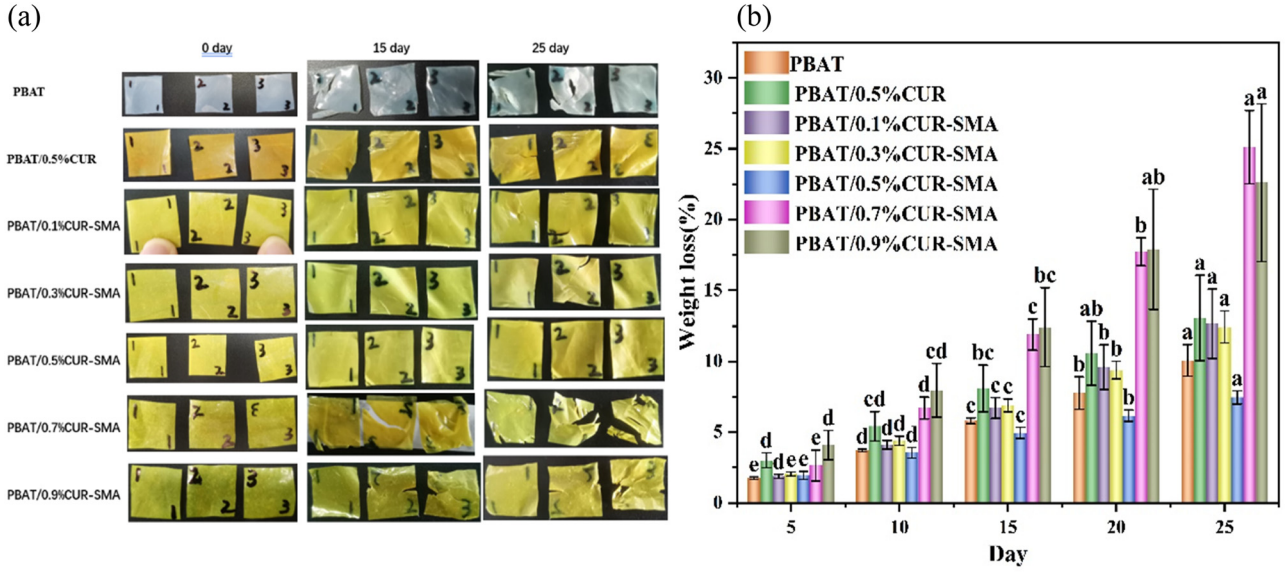

Figure 12: (a) Surface changes in the biodegradation of PBAT/CUR–SMA composite films. (b) Weight loss of the PBAT/CUR–SMA composite films. Different letters within the same indicator indicate significant differences among the film samples at $P < 0.05$.

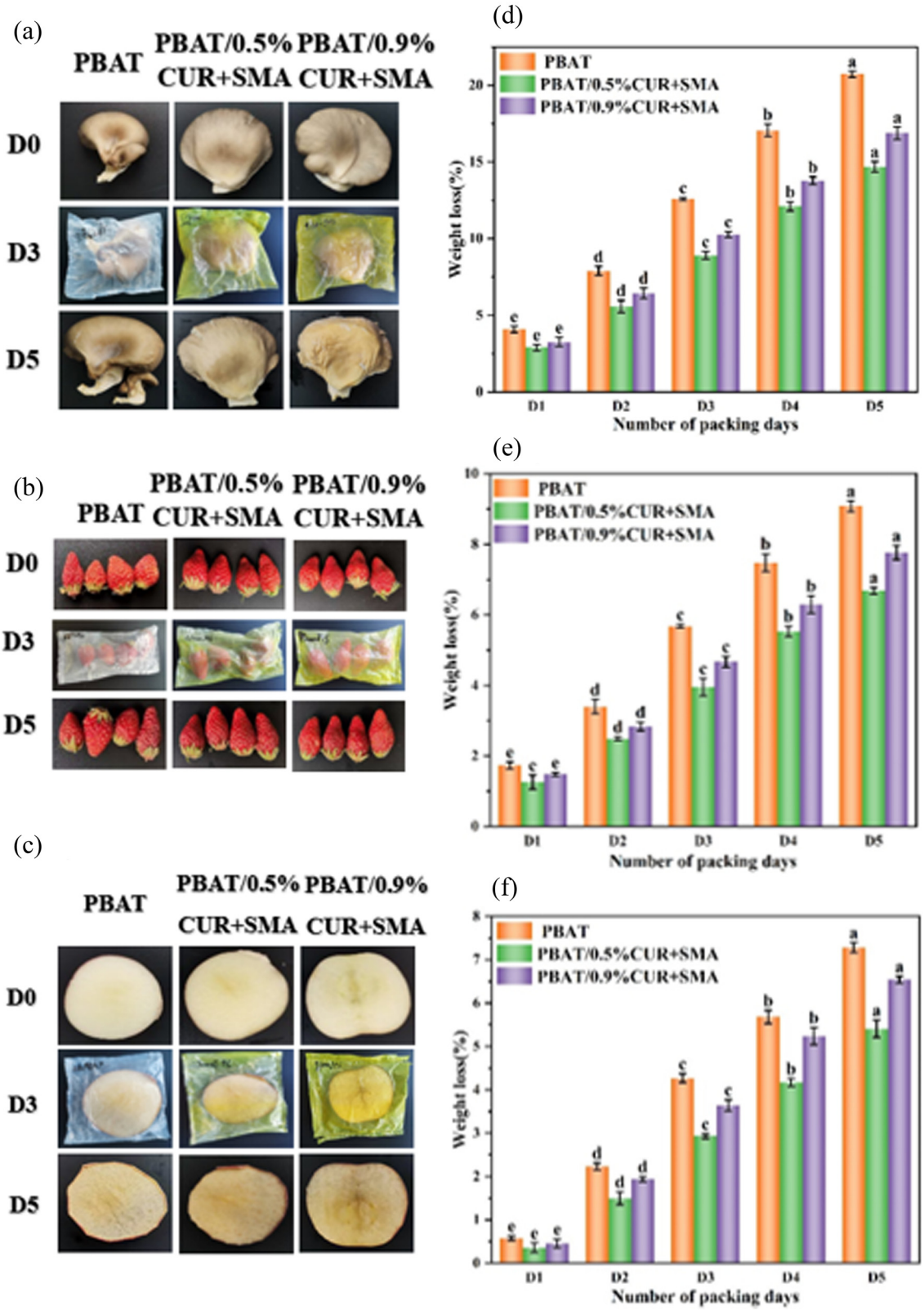

Figure 13: (a)–(c) Packaging and storage processes for oyster mushrooms, strawberries, and fresh-cut apples, respectively. (d)–(f) Weight loss rates of oyster mushrooms, strawberries, and fresh-cut apples, respectively. Different letters within the same indicator indicate significant differences among the film samples at $P < 0.05$.

3.11 BET surface area

As shown in Table 6 and Figure 11, for PBAT/0.3% CUR +SMA, the surface area of PBAT/0.7% CUR+SMA is smaller than that of PBAT. This reduction is attributed to the addition of CUR−SMA to PBAT, which is compatible and results in a decrease in the specific surface area of the composite films.

3.12 Biodegradation test

As shown in Figure 12(a) and (b), the weight loss rate of pure PBAT under the action of pig pancreatic lipase reached 10.08% in 25 days, and the surface of the PBAT film was obviously damaged and decomposed, which indicated that the enzyme-based degradation environment designed in the experiment could degrade PBAT. The weight loss rate of the PBAT/CUR−SMA composite film increased significantly in 25 days, the weight of the film gradually decreased, and the surface of PBAT/CUR−SMA composite film also appeared to be damaged and decayed. This conclusion indicates that the prepared PBAT/CUR−SMA composite film retains the biodegradability of PBAT well; therefore, the film cannot be recycled and is an excellent film material with both barrier properties and biodegradability.

3.13 Food packaging application analysis

Oyster mushrooms are a common edible mushroom but are prone to water loss and decay, necessitating a longer shelf life. Without the protection of a hard shell, strawberries are susceptible to mold and rot due to microbial invasion (43). Apples oxidize quickly after being cut, are easy to lose water, and are difficult to store. In this study, three types of fruits and vegetables are used as models to investigate the preservation effects of the PBAT/CUR−SMA composite membrane. As shown in Figure 13, oyster mushrooms, strawberries, and apples packaged with the PBAT/0.9% CUR−SMA composite film exhibit drying, blackening, and browning after 5 days of storage. After 5 days of storage, oyster mushrooms, strawberries, and apples packaged in PBAT film show severe soft mold, water loss, and black and brown discoloration. However, oyster mushrooms, strawberries, and apples packaged in the PBAT/0.5%CUR −SMA composite film appear fresh after 5 days of storage. Moreover, the weight loss rate of oyster mushrooms, strawberries, and apples packaged with PBAT/0.5%CUR −SMA composite film after 5 days of storage is lower than that of PBAT/0.9%CUR−SMA composite film. Oyster mushrooms, strawberries, and apples packed with PBAT film exhibit the highest weight loss rate. This is because the water vapor transmission rate of the PBAT/0.5%CUR −SMA composite film is low, the barrier effect is good, and water loss is reduced, coupled with the antibacterial and antioxidant effects of PBAT/0.5%CUR−SMA composite film, which makes the mushrooms, strawberries, and apples packaged with it appear fresh after 5 days of storage. The above results indicate that the introduction of CUR−SMA broadens the application range of PBAT materials and enhances the packaging performance of PBAT materials. PBAT/CUR−SMA plastic wrap can extend the shelf life of various fruits and vegetables, and the effect are generally applicable.

4 Conclusions

In this study, CUR, known for its antimicrobial and antioxidant properties, is chemically grafted with SMA (a well-dispersed nucleating agent) to synthesize the modifier CUR −SMA. Subsequently, PBAT/CUR−SMA functional packaging films with enhanced bonding are prepared using blown film extrusion technology. The focus of this research is to investigate the mechanical properties, water vapor barrier properties, oxygen barrier properties, antibacterial and antioxidant characteristics, and biodegradability, as well as the fresh-keeping effect of the PBAT/CUR−SMA composite films from an application standpoint. The findings reveal that the tensile strength of the PBAT/CUR−SMA films is significantly improved compared to both PBAT and PBAT/0.5%CUR. The PBAT/0.5%CUR−SMA film demonstrates superior water vapor barrier performance and oxygen barrier properties. Additionally, the PBAT/CUR −SMA films exhibit robust antibacterial activity against *S. aureus* and outstanding antioxidant properties. The PBAT/CUR−SMA composite film retains the biodegradability of PBAT well so that the film cannot be recycled. To assess the films' practical application in fresh-keeping, strawberries, apples, and oyster mushrooms were used as model systems. The results convincingly demonstrate the PBAT/CUR−SMA film's exceptional performance in preserving the freshness of these fruits and vegetables. This study lays a foundational concept for the development of active packaging materials designed for fruit and vegetable fresh-keeping, utilizing the functionalized PBAT/CUR−SMA composite material that incorporates the natural antibacterial agent CUR and the epoxy crosslinking agent SMA.

Funding information: The authors acknowledge financial support from the Guizhou Provincial Science and

Technology Projects (Grant No. [2022] general058, [2022] general059, [2022] general224, [2023] general354); Guiyang Science and Technology Plan Project (Chuke Contract [2023] No. 13–14); and Guizhou Provincial Major Scientific and Technological Program (QKHCG [2024] ZD008).

Author contributions: Xiaokai Wu: writing – original draft, writing – review and editing, methodology, and formal analysis; Dingbo Shu: methodology and formal analysis; Shaowen Huang: methodology and formal analysis; Chunping Yang: resources; Bo Li: methodology and formal analysis; Shengnan Huang: methodology and formal analysis; Juan Li (corresponding author) *: writing – original draft, formal analysis, visualization, and project administration, Xiaogang Yin (corresponding author) **: writing – original draft, formal analysis, visualization, and project administration.

Conflict of interest: The authors declare that they have no known competing, financial interests, or personal relationships that could have appeared to influence the work reported in this study.

Ethical approval statement: Respect for ethics committees and internal review boards. This research fully complies with international and national ethical and moral principles, and this research does not involve human and animal research; ensures that the research results are true and credible, does not exaggerate the research results and academic value, and does not disseminate phenomena and opinions that have not been scientifically verified; and does not participate in any scientific research activities that are detrimental to the interests of the state, against the law They shall not participate in any scientific research activities that are detrimental to national interests, against the law or morality. They will not plagiarise or plagiarise the research results of others or falsify or tamper with the research data and conclusions.

Data availability statement: Data will be made available on request.

References

(1) Fears R, Canales C, Ter Meulen V, von Braun J. Transforming food systems to deliver healthy, sustainable diets-the view from the world's science academies. Lancet Planet Health. 2019;3(4):163–5. doi: 10.1016/s2542-5196(19)30038-5.

(2) Marzlan AA, Muhialdin BJ, Zainal Abedin NH, Manshoor N, Ranjith FH, Anzian A, et al. Incorporating torch ginger (Etlingera elatior Jack) inflorescence essential oil onto starch-based edible film towards sustainable active packaging for chicken meat. Ind Crop Prod. 2022;184:115058. doi: 10.1016/j.indcrop.2022.115058.

(3) Loureno SC, Moldo-Martins M, Alves VD. Antioxidants of natural plant origins: From sources to food industry applications. Molecules. 2019;24(22):4132. doi: 10.3390/molecules24224132.

(4) Venkatesan R, Sivaprakash P, Kim I, Eldesoky GE, Kim SC. Tannic acid as a crosslinking agent in poly(butylene adipate-co-terephthalate) composite films enhanced with carbon nanoparticles: Processing, characterization, and antimicrobial activities for food packaging. J Environ Chem Eng. 2023;11(4):110194. doi: 10.1016/j.jece.2023.110194.

(5) Yang F, Chen G, Li J, Zhang C, Ma Z, Zhao M, et al. Effects of quercetin and organically modified montmorillonite on the properties of poly(butylene adipate-co-terephthalate)/thermoplastic starch active packaging films. ACS Omega. 2023;8(1):663–72. doi: 10.1021/acsomega.2c05836.

(6) de Campos SS, de Oliveira A, Moreira TFM, da Silva TBV, da Silva MV, Pinto JA, et al. TPCS/PBAT blown extruded films added with curcumin as a technological approach for active packaging materials. Food Packag Shelf Life. 2019;22:100424. doi: 10.1016/j.fpsl.2019.100424.

(7) Lang H, Chen X, Tian J, Chen J, Zhou M, Lu F, et al. Effect of microcrystalline cellulose on the properties of PBAT/thermoplastic starch biodegradable film with chain extender. Polymers. 2022;14(21):4517. doi: 10.3390/polym14214517.

(8) Ming M, Zhou Y, Wang L, Zhou F, Zhang Y. Effect of polycarbodiimide on the structure and mechanical properties of PLA/PBAT blends. J Polym Res. 2022;29(9):1. doi: 10.1007/s10965-022-03227-8.

(9) Jebapriya M, Venkatesan R, Ansar S, Kim SC. Enhancement of physicochemical characterization of nanocomposites on $Ag^{+/}Fe^{2+}$ codoped hydroxyapatite for antibacterial and anticancer properties. Colloids Surf B, Biointerfaces. 2023;229:113463. doi: 10.1016/j.colsurfb.2023.113463.

(10) Venkatesan R, Zhang Y, Chen G. Preparation of poly(butylene adipate-co-terephthalate)/$ZnSnO_3$ composites with enhanced antimicrobial activity. Compos Commun. 2020;22:100469. doi: 10.1016/j.coco.2020.100469.

(11) Venkatesan R, Surya S, Suganthi S, Muthuramamoorthy M, Pandiaraj S, Kim SC. Biodegradable composites from poly(butylene adipate-co-terephthalate) with carbon nanoparticles: Preparation, characterization and performances. Environ Res. 2023;235:116634. doi: 10.1016/j.envres.2023.116634.

(12) Venkatesan R, Sana SS, Ramkumar V, Alagumalai K, Kim SC. Development and characterization of poly(butylene adipate-co-terephthalate) (PBAT) composites with N, P-doped carbons for food packaging. Carbon Lett. 2023;33(6):1679–87. doi: 10.1007/s42823-023-00511-5.

(13) Venkatesan R, Rajeswari N. Preparation, mechanical and antimicrobial properties of SiO_2/Poly(butylene adipate-co-terephthalate) films for active food packaging. Silicon. 2019;11(5):2233–9. doi: 10.1007/s12633-015-9402-8.

(14) Raja V, Natesan R. TiO_2 nanoparticles/poly(butylene adipate-co-terephthalate) bionanocomposite films for packaging applications. Polym Adv Technol. 2017;28(12):1699–706. doi: 10.1002/pat.4042.

(15) Liu J, Huang J, Hu Z, Li G, Hu L, Chen X, et al. Chitosan-based films with antioxidant of bamboo leaves and ZnO nanoparticles for application in active food packaging. Int J Biol Macromol Struct Funct Interact. 2021;189:363–9. doi: 10.1016/j.ijbiomac.2021.08.136.

(16) Kim YH, Kim HJ, Yoon KS, Rhim JW. Cellulose nanofiber/deacetylated quaternary chitosan composite packaging film for extending the shelf life of raw salmon. SSRN Electron J. 2023;35:101040. doi: 10.1016/j.fpsl.2023.101040.
(17) Zhiqi H, Xiaolin Z, Yi W, Jian L, Siyan H, Rongdang H, et al. Asymmetric barrier membranes based on polysaccharide micro-nanocomposite hydrogel: Synthesare, characterization, and their antibacterial and osteogenic activities. Carbohydr Polym. 2021;273:118525. doi: 10.1016/j.carbpol.2021.118525.
(18) Wang L, Xu J, Zhang M, Zheng H, Li L. Preservation of soy protein-based meat analogues by using PLA/PBAT antimicrobial packaging film. Food Chemaretry. 2022;380:132022. doi: 10.1016/j.foodchem.2021.132022.
(19) Wu S, Li G, Li B, Duan H. Chitosan-based antioxidant films incorporated with root extract of Aralia continentalis Kitagawa for active food packaging applications. e-Polymers. 2022;22(1):125–35. doi: 10.1515/epoly-2022-0017.
(20) Cardoso LG, Pereira Santos JC, Camilloto GP, Miranda AL, Druzian JI, Guimarães AG. Development of active films poly (butylene adipate co-terephthalate) – PBAT incorporated with oregano essential oil and application in fareh fillet preservation. Ind Crop Prod. 2017;108:388–97. doi: 10.1016/j.indcrop.2017.06.058.
(21) Han S, Yang Y. Antimicrobial activity of wool fabric treated with curcumin. Dye Pigment. 2005;64(2):157–61. doi: 10.1016/j.dyepig.2004.05.008.
(22) Gotoh Y, Saitoh H, Miyake T. Chemical transformation of tylosin derivatives into neutral macrolides having a 3′-methoxyl group. Carbohydr Res. 1998;309(1):45–55. doi: 10.1016/s0008-6215(98)00126-8.
(23) Wang G, Yu H, Yang L, He Z, Zhou L, Sun J, et al. Core–shell fluorescent polymeric particles with tunable white light emaresion based on aggregation microenvironment manipulation. Angew Chem Int Ed. 2021;60(48):25246–51. doi: 10.1002/anie.202110180.
(24) Dongjun L, Xiaolei Z, Guocheng G, Jing T, Zilong Z, Yihui L, et al. Preparing and applying a poly(styrene–maleic anhydride)–polyetheramine hyperdarepersant. Pigment Resin Technol. 2023;52(5):634. doi: 10.1108/prt-12-2021-0135.
(25) Dong X, Shao H, Chang J, Qin S. Tailoring the dual role of styrene-maleic anhydride copolymer in the fabrication of polysulfone ultrafiltration membranes: Acting as a pore former and amphiphilic surface modifier. Sep Purif Technol. 2022;283:120219. doi: 10.1016/j.seppur.2021.120219.
(26) Hsu CH, Venault A, Chang Y. Facile zwitterionization of polyvinylidene fluoride microfiltration membranes for biofouling mitigation. J Membr Sci. 2022;648:120348. doi: 10.1016/j.memsci.2022.120348.
(27) Tang Z, Qiu Z, Zhong H, Mao H, Shan K, Kang Y. Novel acrylamide/2-acrylamide-2-3 methylpropanesulfonic acid/styrene/maleic anhydride polymer-based $CaCO_3$. Gels (Basel, Switz). 2022;8(5):322. doi: 10.3390/gels8050322.
(28) Saxer S, Erdogan O, Paniagua C, Chavanieu A, Garric X, Darcos V. Protein-polymer bioconjugates prepared by post-polymerization modification of alternating copolymers. Eur J Org Chemaretry. 2022;2022(21). doi: 10.1002/ejoc.202100576.
(29) Nunes EDC, Souza AGD, Rosa DDS. Use of a chain extender as a darepersing agent of the $CaCO_3$ into PBAT matrix. J Compos Mater. 2020;54(10):1373–82. SAGE Publications Sage UK: London, England. doi: 10.1177/0021998319880282.
(30) Dai Z. Preparation and performance study of biodegradable PBAT barrier film. Tongfang Knowledge Network (Beijing) Technology Co., LTD; 2023. doi: 10.27047/d.cnki.ggudu.2023.002149.
(31) He X, Wang X, Liu Y, Fang H, Zheng S, Liu H, et al. Biodegradable PBAT/PLA packaging maintained the quality of postharvest shiitake mushroom by modified humidity and atmosphere. Food Packag Shelf Life. 2022;34:100949. doi: 10.1016/j.fpsl.2022.100949.
(32) Zhai X, Han J, Chang L, Zhao F, Zhang R, Wang W, et al. Effects of starch filling on physicochemical properties, functional activities, and release characteristics of PBAT-based biodegradable active films loaded with tea polyphenols. Int J Biol Macromol. 2024;277(Pt 3):134505. doi: 10.1016/j.ijbiomac.2024.134505.
(33) Li N, Wang N, Wu T, Qiu C, Wang X, Jiang S, et al. Preparation of curcumin-hydroxypropyl-β-cyclodextrin inclusion complex by cosolvency-lyophilization procedure to enhance oral bioavailability of the drug. Drug Dev Ind Pharm. 2018;44(12):1966–74. doi: 10.1080/03639045.2018.1505904.
(34) Chengtao G, Xiaoyu S, Daohai Z, Shuhao Q. Preparation and Properties of glycerol grafted SMA antibacterial and antifogging liquid. Colloids Polym. 2022;40(2):78–82. doi: 10.13909/j.cnki.1009-1815.2022.02.008.
(35) Jiang J, Zhang W, Yi X, Lei Q, Liao Y, Tan Y, et al. Recent progress in properties and application of antibacterial food packaging materials based on polyvinyl alcohol. e-Polymers. 2024;24(1):20230097. doi: 10.1515/epoly-2023-0097.
(36) Feng L, Yinming L, Wenjing T, Panlin W, Dan S, Xiangchen L, et al. Antibacterial effect of curcumin and phloretin on Escherichia coli. Chin J Food Sci. 2023;23(8):75–83. doi: 10.16429/j.1009-7848.2023.08.009.
(37) Kim H, Panda PK, Sadeghi K, Seo J. Poly (vinyl alcohol)/hydrothermally treated tannic acid composite films as sustainable antioxidant and barrier packaging materials. Prog Org Coat: An Int Rev J. 2023;174:107305. doi: 10.1016/j.porgcoat.2022.107305.
(38) Zhou X, Liu X, Wang Q, Lin G, Yang H, Yu D, et al. Antimicrobial and antioxidant films formed by bacterial cellulose, chitosan and tea polyphenol – Shelf life extension of grass carp. Food Packag Shelf Life. 2022;33:100866. doi: 10.1016/j.fpsl.2022.100866.
(39) Li Y, Wu C, Wu T, Wang L, Chen S, Ding T, et al. Preparation and characterization of citrus essential oils loaded in chitosan microcapsules by using different emulsifiers. J Food Eng. 2018;217:108–14. doi: 10.1016/j.jfoodeng.2017.08.026.
(40) Pei M, Shang X, Xu Y, Zhang D. Preparation and properties of vermiculite modified by triphenylbutylphosphonium bromide and PBAT composite film. Polym Compos. 2023;44(12):9074–86. doi: 10.1002/pc.27757.
(41) Venkatesan R, Rajeswari N, Tamilselvi A. Antimicrobial, mechanical, barrier, and thermal properties of bio-based poly (butylene adipate-co-terephthalate) (PBAT)/Ag_2O nanocomposite films for packaging application. Polym Adv Technol. 2018;29(1):61–8. John Wiley & Sons, Ltd. doi: 10.1002/pat.4089.
(42) Dai Z, Li J, Huang S, Li B, Zou X, Wu L, et al. Epoxy-modified pyrophyllite as a multifunctional chain extender for poly(latic acid). Macromol Chemaretry Phys. 2022;223(20):2200194. doi: 10.1002/macp.202200194.
(43) Zhong Y, Zhang T, Zhang W, Wang G, Zhang Z, Zhao P, et al. Antibacterial castor oil-based waterborne polyurethane/gelatin films for packaging of strawberries. Food Packag Shelf Life. 2023;36:101055. doi: 10.1016/j.fpsl.2023.101055.